

Zero-shot Sim2Real Adaptation Across Environments

Buddhika Laknath Semage*, Thommen George Karimpanal, Santu Rana,
Svetha Venkatesh
Applied Artificial Intelligence Institute
Deakin University
Geelong, Australia
*Email: bsemage@deakin.edu.au

February 9, 2023

Abstract

Simulation based learning often provides a cost-efficient recourse to reinforcement learning applications in robotics. However, simulators are generally incapable of accurately replicating real-world dynamics, and thus bridging the sim2real gap is an important problem in simulation based learning. Current solutions to bridge the sim2real gap involve hybrid simulators that are augmented with neural residual models. Unfortunately, they require a separate residual model for each individual environment configuration (i.e., a fixed setting of environment variables such as mass, friction etc.), and thus are not transferable to new environments quickly. To address this issue, we propose a Reverse Action Transformation (RAT) policy which learns to imitate simulated policies in the real-world. Once learnt from a single environment, RAT can then be deployed on top of a Universal Policy Network to achieve zero-shot adaptation to new environments. We empirically evaluate our approach in a set of continuous control tasks and observe its advantage as a few-shot and zero-shot learner over competing baselines.

1 Introduction

In recent years, deep reinforcement learning (RL) has been successfully used to solve a number of complex physics related problems such as solving a Rubik’s Cube with a robotic hand [4], manoeuvring objects [20], etc. To circumvent the sample inefficiency of deep learning methods used in these applications, many of them use numerical physics-based simulators to generate cheaper, synthetic experiences. Simulation-based learning methods such as Universal Policy Networks (UPNs)[35] additionally offer the benefit of learning a range of policies across different environmental configurations (e.g., mass, friction, etc.,) at one go, enabling quick adaptability if the environment parameters change. However, the exact replication of real-world dynamics in simulators is challenging due to the existence of environment-specific transient dynamic

factors (e.g., air-resistance), which can be either exceptionally hard or too computationally intensive to be modelled. Due to such discrepancies between the simulator and real-world dynamics (i.e., reality-gap), policies learnt in simulators generally do not perform well when they are directly transferred to the real-world.

To bridge this reality-gap, hybrid simulators consisting of both numerical as well as neural components have been studied by [3, 2, 18, 7]. While these approaches have been shown to bridge the reality-gap, they are designed to be trained separately for each individual real-world environment, and have to be retrained when the environment parameters change. *Action Transformation (AT)* policy by [14, 9, 19] learns to transform actions in the simulator to mimic the state transitions in the real world, thereby, making the learnt policy applicable to the real world. However, they are not compatible with pretrained policies such as UPNs because task-policies need to be learnt on the transformed action set, which limits the adaptability of the agent. Thus, learning to bridge the reality-gap for a range of environmental settings without retraining is still an open problem.

To address these shortcomings, we propose a *Reverse Action Transformation (RAT)* policy that combines the adaptability of UPN with the concept of action transformation. Figure 1 shows how a golf-playing robot can bridge the sim-to-real gap using corrective actions from the *RAT* policy. Instead of learning to reproduce real-world dynamics in the simulator as done in *GAT* [15], in *RAT*, we aim to learn the reverse transformation — making real-world trajectories mimic the optimal trajectories learnt in the simulator. If the reality-gap remains fixed locally across adjacent environment configurations, *RAT* policies learnt in one environment will also transfer to those adjacent environments, making the combination of UPN+*RAT* a vehicle for adaptable reality-gap-free policy learning. We add that our use of ‘reality-gap-free’ learning utilises the predictability of the agent, as the agent will see the real-world as a simulator and thus would be able to take predictable optimal actions as per its simulation-learnt policy. Even though such a policy may be slightly suboptimal (e.g., if the reality-gap helps to discover a better policy), it makes our learning robust to test time changes in the environment configuration. Specifically, we first train a UPN on a relatively small number of simulator parameters to learn optimal simulated policies (step 1, Fig. 1), which may not transfer well to the real-world (step 2, Fig. 1). Next, we train *RAT* by sampling different reality-gap transitions in the simulator to learn a robust initial policy. Initialised with this policy, we then deploy the combination of UPN+*RAT* policy in the real-world to bridge the reality-gap (step 3, Fig. 1). Subsequently, when an environment change is detected (e.g., change in ground friction due to rain), we appropriately set the parameter of the UPN for the new environment and use the UPN+*RAT* without any retraining to achieve zero-shot adaptation (Step 4, Fig. 1). One of the key intuitions behind learning *RAT* is that in the presence of moderate reality gaps, it would be relatively more sample efficient to learn an explicit mapping from simulated policies to their ideal real-world counterparts, as opposed to adapting each task-specific simulation policy to the real-world. Experiments on six continuous control tasks show that our approach outperforms other UPN-based adaptable baselines.

In summary, the main contributions of our study are:

1. Proposing *Reverse Action Transformation (RAT)*, an adaptable policy that can

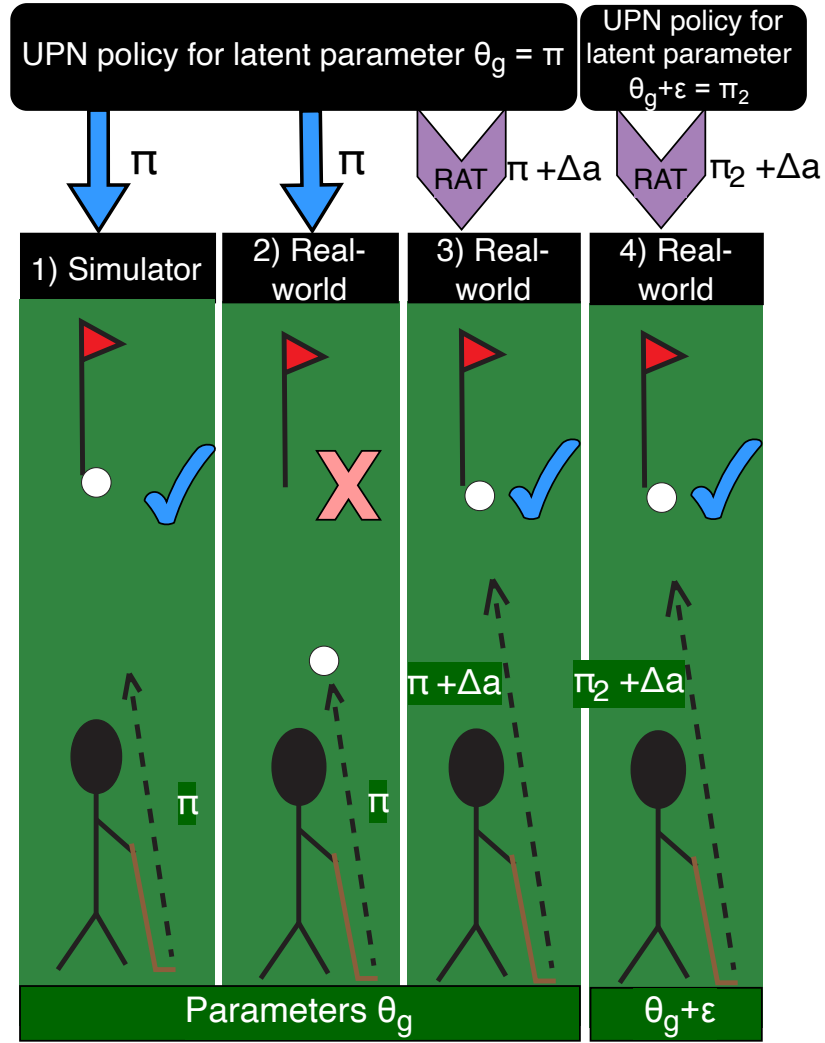


Figure 1: Combining *RAT* with a UPN for fast adaptability of pretrained simulated policies to real-world conditions. For a task of golf played under known modellable latent parameters θ_g (e.g., friction), (1) the optimal simulated policy π from UPN for parameters θ_g achieves the task in the simulator. (2) When the same policy π is transferred to the real-world, due to the reality gap (e.g., rolling friction in the real-world) the simulated policy does not achieve the task. (3) *RAT* transforms policy π such that the resulting trajectory, when rolled out in the real-world, matches the simulated trajectory through a Δa correction in the action. (4) For an adjacent environment with latent parameters $\theta_g + \epsilon$, the respective UPN policy π_2 is transformed by *RAT* using the same Δa correction.

correct real-world policies to follow optimal simulated trajectories learnt from a Universal Policy Network.

2. Formulating and implementing *RAT* policy with a robust initial policy to improve the sample efficiency of learning.
3. Empirically demonstrating improved real-world transfer on a set of continuous control tasks.

2 Background

Simulators are a cheap source of synthetic data to alleviate the sample inefficiency of deep learning methods [22] that are being used with many RL applications today. However, for successful sim2real transfer, simulation parameters (e.g., friction, restitution) often need to be tuned to match the real-world dynamics (i.e., system identification or grounding). A relatively simple basis for this is to simply minimise the differences between the simulation and real-world trajectories [1, 38, 8, 11, 5, 6]. Direct policy search is another approach for system identification, where optimal simulation parameters are discovered by evaluating simulated policies in the real-world to find the parameters corresponding to the highest performing simulated policy [12, 35, 34, 33, 16].

Many direct policy search methods, although imperfect at modelling the real-world, carry the benefit of adaptability due to their maintenance of many pretrained simulation policies which are directly transferable to the real-world after the grounding process. In this light, Universal Policy Networks (UPN) [35] has become a useful tool, as it offers a framework for learning policies for a continuous range of simulation parameters by training only on a limited set of parameters. With such a trained UPN, neural networks [35], Bayesian Optimisation [33] and evolutionary algorithms [34] can be used to efficiently search for an optimal set of parameters that yield the best policy to be transferred to the real-world. For the purpose of this study, we assume the knowledge of real-world parameter values and thus, obviate the grounding process from both our method and the baselines.

In addition to grounding, hybrid simulators examine combining numerical simulators with neural components to reduce the mismatch in the dynamics of the simulator and the real-world [3, 2, 7, 13, 17]. Although they have been shown to improve modelling capabilities compared to analytical simulators, since the focus is to solely improve the dynamics mismatch, policies learnt on such hybrid simulators would need to be re-trained when the residual layer, which models factors such as air resistance or rolling friction, changes. Given that such factors are usually highly transient, frequent changes to the residual layer would be needed. As such, policies trained on hybrid simulators are ill-equipped for learning adaptable policies under changing environment conditions. Residual policies [30, 36, 18] follow a similar concept, where a classical controller is augmented with a correction policy in the real-world using the task reward. Since they learn a policy corresponding to a single parameter setting, this solution is also not adaptable when the environment conditions change.

Instead of trying to replicate real-world dynamics through the transition function, *Grounded Action transformation (GAT)* [15] and other related approaches [9, 19, 37,

10] directly modified the simulated policy to match the dynamics of the real-world. In these works, the simulator is grounded to follow the real-world using the learnt action mappings. While our study was inspired from this line of research, we try to address several drawbacks with *GAT*: 1) These works are incompatible with pretrained policies (e.g., universal policies), because the simulated task policies need to be learnt on transformed actions, 2) Since the simulator’s state space can be more limited than that of the real-world, trying to imitate the real-world using such a simulator can lead to subpar results, 3) deploying these methods on unknown environments with a different reality-gap will require the action mappings to be updated, which in turn will require re-learning of the task policies. In contrast to this, we enable the same policies to be retained, requiring adaptation of just the *RAT* policy, which is significantly easier to train.

Learning simulated policies robust to real-world noise is another approach related to our work. Domain randomisation (DR) [31, 26, 29, 24, 23, 27, 21, 4, 25] has become a common approach, where a robust policy is learnt by training on a range of parameters. While it provides a relatively convenient approach for sim2real transfer without specifically grounding the simulator, the performance of a DR policy heavily relies on the parameter distribution on which it was trained. Particularly, when the parameter range is large, DR policies have been known to produce extremely conservative policies[29] compared to regular policies.

3 Method

In this study, we propose a mechanism to bridge the reality-gap by learning a policy to correct a pretrained simulation policy, such that the corrected policy produces real-world trajectories that closely match the optimal trajectory learnt in the simulator. The simulated environment ψ^{sim} is parameterised by modellable latent parameters θ for which we can model accurate simulation dynamics using standard numerical simulators without extensive computational costs. The real-world ψ is parameterised by $\phi = [\theta, U]$ ($\theta, U \in \mathbb{R}^d$), where U represents unmodellable parameters that are difficult to be modelled universally (e.g., air-resistance, rolling friction). Learning tasks in the simulator and the real-world are represented as MDPs $\mathcal{M}_{sim} = \langle \mathcal{S}, \mathcal{A}, \mathcal{T}_{sim}, \theta, \mathcal{R} \rangle$ and $\mathcal{M} = \langle \mathcal{S}, \mathcal{A}, \mathcal{T}, \phi, \mathcal{R} \rangle$ respectively, where \mathcal{S} is the state space, \mathcal{A} is the action space, \mathcal{T}_{sim} and \mathcal{T} are respectively the simulation and real-world transition functions with $\mathcal{S} \times \mathcal{A} \rightarrow \mathcal{S}$ mappings and $\mathcal{R} : \mathcal{S} \times \mathcal{A} \rightarrow \mathbb{R}$ is the reward function.

Under this formulation, we utilise an RL agent design commonly known as Universal Policy Network (UPN) to learn in simulation, a large range of policies corresponding to different latent parameter configurations. A UPN is learned on the MDP \mathcal{M}_{sim} by sampling parameters θ in the simulation and learning a policy network capable of providing policies conditioned on latent parameters θ . To achieve this goal, UPN’s state is constructed by appending the task’s observable state (e.g., object positions, velocities) with the sampled θ (e.g., friction, restitution) values in a given range. The UPN is then trained in simulation with RL to learn policies over the range of the provided latent parameter values, while also generalising to unseen latent parameters in the range.

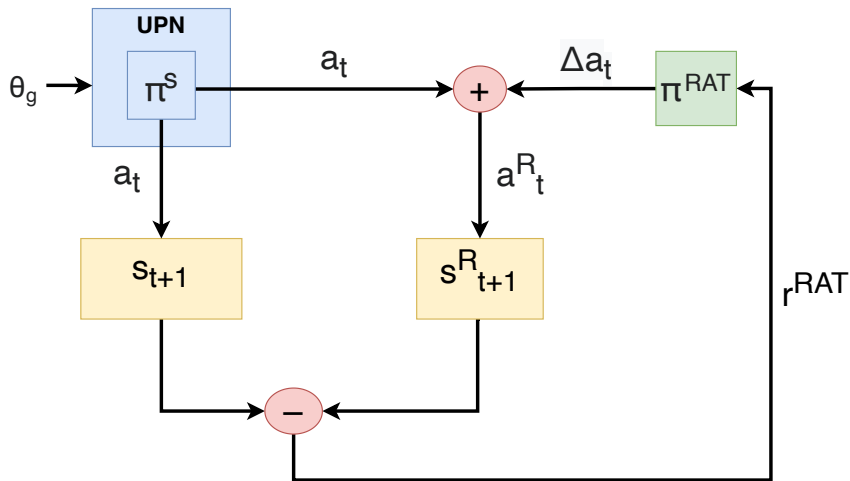


Figure 2: The process of learning Reverse Action Transformation (RAT). The RAT policy π^{RAT} outputs Δa_t which is the amount of adjustment needed on the UPN π^S action a_t (conditioned by latent parameter θ_g) to follow the simulated trajectory in the real-world. The adjusted action a_t^R is executed in the real-world which results in the state s_{t+1}^R . The difference between the simulator’s s_{t+1} state after executing a_t and the real-world’s s_{t+1}^R is used as a negative reward r^{RAT} in learning π^{RAT} .

In this workflow, we first pretrain a UPN, and aim to appropriately correct a suitable policy drawn from it, so that the resulting policy produces desirable trajectories in a previously unseen real-world. For this purpose, we learn a *Reverse Action Transformation (RAT)* policy that appropriately corrects the simulated policy to reproduce the corresponding desired simulated trajectory in the real-world (Fig. 2). RAT would then transfer to span other environments (with slightly different latent parameters) as long as the reality-gap remains the same.

3.1 Reverse Action Transformation (RAT) Policy

One of the key intuitions behind learning RAT is that in the presence of large reality gaps, it would be relatively more sample efficient to learn an explicit mapping from simulated policies to their ideal real-world counterparts, as opposed to adapting each task-specific simulation policy to the real-world. For a measured ground truth modellable latent parameter $\theta_g \in \theta$ and an unknown reality-gap $\mu_g \in U$, we learn a correction policy $\pi_{\theta_g, \mu_g}^{RAT}$ in a real-world ψ_{ϕ_g} (parameterised by $\phi_g = [\theta_g, \mu_g]$) which when employed in conjunction with the UPN, imitates the UPN’s θ_g conditioned policy $\pi_{\theta_g}^S$ learnt in a simulated environment $\psi_{\theta_g}^{sim}$. This approach is similar to the idea of *Action Transformations (AT)* [14, 9, 19], but instead of learning a simulated policy to reproduce the real-world trajectories, we learn the reverse (hence the name *Reverse Action Transform*), by learning corrections to the trained simulation policy $\pi_{\theta_g}^S$ in order to reproduce the corresponding simulated trajectories in the real-world (Fig. 2).

To closely emulate simulated trajectories in the real-world through *RAT*, we assume the existence of such a real-world policy. Secondly, for the purpose of this study, we assume ground truth latent parameters of the original environment and environments corresponding to adjacent latent parameter configurations to be known, perhaps through direct measurements and/or policy search based grounding methods [12, 38].

We learn the *RAT* policy through RL by defining an additional MDP framework: $\mathcal{M}^{\mathcal{RAT}} = \langle \mathcal{S}^{\mathcal{RAT}}, \mathcal{A}^{\mathcal{RAT}}, \mathcal{T}^{\mathcal{RAT}}, \mathcal{R}^{\mathcal{RAT}}, \theta, U \rangle$ where $\mathcal{S}^{\mathcal{RAT}}$ is the *RAT* state space, $\mathcal{A}^{\mathcal{RAT}}$ is the *RAT* action space, $\mathcal{T}^{\mathcal{RAT}} : \mathcal{S}^{\mathcal{RAT}} \times \mathcal{A}^{\mathcal{RAT}} \rightarrow \mathcal{S}^{\mathcal{RAT}}$ is the *RAT* transition function and $\mathcal{R}^{\mathcal{RAT}} : \mathcal{S}^{\mathcal{RAT}} \times \mathcal{A}^{\mathcal{RAT}} \rightarrow \mathbb{R}$ is the reward function used to train the *RAT* policy. The state $s_t^{\mathcal{RAT}} \in \mathcal{S}^{\mathcal{RAT}}$ at a given timestep t is constructed by concatenating the real-world state $s_t^R \in \mathcal{S}$ with the greedy action of the trained simulation policy obtained from the UPN.

$$s_t^{\mathcal{RAT}} = [s_t^R, \pi_{\theta_g^S}(s_t)]$$

Instead of directly imitating the simulated policy $\pi_{\theta_g^S}$, *RAT* follows an approach inspired by [19], by predicting the difference of actions $\Delta a_t \in \mathcal{A}^{\mathcal{RAT}}$ between the simulated and the real-worlds. [19] suggested that such an approach improved learning due to the normalising effect on the action output space of the corresponding neural network.

As explained later in Eq. 2, the reward function for training *RAT* is determined by measuring the distance between the simulated and real-world states when the corresponding actions are taken. While the simulated action is determined by $\pi_{\theta_g^S}$, the real-world action a_t^R is determined by adjusting the action from the simulated policy $\pi_{\theta_g^S}$ by the corresponding *RAT* action Δa_t for that *RAT* state $s_t^{\mathcal{RAT}}$:

$$\begin{aligned} \Delta a_t &\leftarrow \pi_{\theta_g, \mu_g}^{\mathcal{RAT}}(s_t^{\mathcal{RAT}}) \\ a_t^R &= \pi_{\theta_g^S}(s_t) + \Delta a_t \end{aligned} \tag{1}$$

We execute the action a_t^R in the real-world and the UPN policy $\pi_{\theta_g^S}(s_t)$ in the simulated world to transit to the states in next timestep $t + 1$. Then, the squared Euclidean distance between the real-world’s state s_{t+1}^R and simulated environment’s state s_{t+1} in timestep $t + 1$ is computed as a negative reward $r^{\mathcal{RAT}} \in \mathcal{R}^{\mathcal{RAT}}$ for training *RAT*.

$$r^{\mathcal{RAT}} = -|s_{t+1}^R - s_{t+1}|_2^2 \tag{2}$$

Following the above steps iteratively, the *RAT* policy $\pi_{\theta_g, \mu_g}^{\mathcal{RAT}}$ learns to produce the appropriate correction Δa_t to produce simulation-like trajectories in the real-world. *RAT* policy training is detailed in Algorithm 1.

3.2 Robust *RAT* Initialisation

As the reality-gap in the real-world is unknown, we require the initial *RAT* policy to be robust to span different possible reality-gap values. To incorporate this property, we use domain randomisation in the simulator to learn a robust *RAT* initial policy $\bar{\pi}_{\theta_g}^{\mathcal{RAT}}$ by training it using a range of reality-gaps. For a defined l lower and h upper limits,

Algorithm 1 *RAT* Policy Training (*Train_RAT_Policy*)

Input:

- 1: θ_g - ground-truth modellable parameters
 - 2: μ_g - ground-truth unmodellable parameters (unknown)
 - 3: π^S - a trained UPN for the task
 - 4: ψ_ϕ - real-world, $\psi_{\theta_g}^{sim}$ - a parameterisable simulator
 - 5: *reset* - simulator reset at each step?
 - 6: **Output:** Trained *RAT* correction policy $\pi_{\theta_g, \mu_g}^{RAT}$
 - 7:
 - 8: **if** a *RAT* initial policy given **then**
 - 9: Initialise *RAT* policy $\pi_{\theta_g, \mu_g}^{RAT} \leftarrow$ *RAT* initial policy
 - 10: **else**
 - 11: Initialise *RAT* policy $\pi_{\theta_g, \mu_g}^{RAT} \leftarrow \emptyset$
 - 12: **end if**
 - 13: $s_t^R \leftarrow$ Initialise state from real-world task ψ_ϕ
 - 14: $s_t \leftarrow s_t^R$, $\psi_{\theta_g}^{sim}$ state $\leftarrow s_t^R$
 - 15: **for** Each step of the episode **do**
 - 16: //Get UPN action for the state s_t and latent parameters θ_g
 - 17: $a_t \leftarrow \pi_{\theta_g}^S(s_t)$
 - 18: $s_{t+1} \leftarrow$ Execute a_t in simulator $\psi_{\theta_g}^{sim}$
 - 19: //Get *RAT* corrected action
 - 20: $a_t^R \leftarrow a_t + \pi_{\theta_g, \mu_g}^{RAT}(s_t^{RAT} = [s_t^R, a_t])$
 - 21: $s_{t+1}^R \leftarrow$ Execute a_t^R in the real-world ψ_ϕ
 - 22: $\pi_{\theta_g, \mu_g}^{RAT} \leftarrow$ Use s_{t+1} , s_{t+1}^R with Eq. 2 to calculate the reward and update *RAT* policy using the selected RL algorithm
 - 23: $s_t^R \leftarrow s_{t+1}^R$
 - 24: **if** *reset* **then**
 - 25: //Change simulator's state to real-world state
 - 26: $\psi_{\theta_g}^{sim}$ state $\leftarrow s_t^R$, $s_t \leftarrow s_t^R$
 - 27: **else**
 - 28: $s_t \leftarrow s_{t+1}$
 - 29: **end if**
 - 30: **end for**
-

we uniformly sample a simulated reality gap value $\bar{\mu} \sim Uniform(l, h)$, $\bar{\mu} \in U$ in each episode, using which we model a hypothetical real-world $\psi_{\bar{\phi}}$ parameterised by $\bar{\phi} = [\theta_g, \bar{\mu}]$. Using $\psi_{\bar{\phi}}$ and its transition function \bar{T} , the subsequent hypothetical real-world state \bar{s}_{t+1}^R is given as.

$$\bar{s}_{t+1}^R \leftarrow \bar{T}(s_t, \bar{a}_t), \quad (3)$$

Here, \bar{a} is the corrected action obtained using robust *RAT* initial policy $\bar{\pi}_{\theta_g}^{RAT}$,

$$\bar{a}_t \leftarrow a_t + \bar{\pi}_{\theta_g}^{RAT}(\bar{s}_t^{RAT} = [s_t, a_t]),$$

where a_t is the UPN action corresponding to ground truth latent parameters θ_g , which produces state $s_{t+1} \leftarrow \mathcal{T}_{sim}(s_t, a_t)$ from state s_t . The obtained states \bar{s}_{t+1}^R and s_{t+1} are used to obtain the reward (as in Eq. 2) for training the *RAT* initial policy.

The steps for training the *RAT* initial policy are given in Algorithm 2. Once trained, the *RAT* initial policy is used as the initial estimate of the *RAT* policy when used in a real-world environment. Depending on the availability of a real-world interaction budget, the *RAT* policy then can be improved (i.e., adapted) from real-world interactions as an optional few-shot learning workflow (not explored in this study).

Algorithm 2 Robust *RAT* Initial Policy Training (*Train_RAT_Initial_Policy*)

Input:

- 1: M - number of sim. episodes to run
 - 2: l, h - lower and upper bounds for reality-gap sampling
 - 3: θ_g - ground-truth modellable parameters
 - 4: $\psi_{\theta}^{sim}, \bar{\psi}_{\bar{\phi}}^{sim}$ - two parameterisable simulators
 - 5: **Output:** Trained robust *RAT* initial policy $\bar{\pi}_{\theta_g}^{RAT}$
 - 6:
 - 7: Initialise *RAT* *initial* policy $\bar{\pi}_{\theta_g}^{RAT} \leftarrow \emptyset$
 - 8: **for** $m \leftarrow 1$ to M **do**
 - 9: $\bar{\mu} \sim Uniform(l, h)$ //sample a reality-gap value
 - 10: $\bar{\phi} = [\theta_g, \bar{\mu}]$
 - 11: Parameterise simulator $\bar{\psi}_{\bar{\phi}}^{sim}$ with sampled $\bar{\phi}$
 - 12: Reset simulator $\bar{\psi}_{\bar{\phi}}^{sim}$ to a random initial state
 - 13: //Train *RAT* initial policy using standard *RAT* training routine (Algo. 1), but with $\bar{\psi}_{\bar{\phi}}^{sim}$ set as the real-world ψ_{ϕ} and *RAT* policy $\pi_{\theta_g, \mu_g}^{RAT}$ initialised with the policy $\bar{\pi}_{\theta_g}^{RAT}$
 - 14: $\bar{\pi}_{\theta_g}^{RAT} \leftarrow Train_RAT_Policy(\psi_{\theta}^{sim}, \bar{\psi}_{\bar{\phi}}^{sim}, \bar{\pi}_{\theta_g}^{RAT})$
 - 15: **end for**
-

3.3 Zero-shot Transfer in Adjacent Environments

Once *RAT* initial policy is learnt in simulation, we examine whether it can be used in adjacent environments where the reality-gap stays consistent (i.e., zero-shot transfer).

For this purpose, we consider a modellable latent parameter setting $\hat{\theta}$ that is ϵ -close ($\epsilon < \epsilon_{max}$) to the original ground truth parameters θ_g , while the reality-gap between the simulator and the real-world μ_g remains consistent for both environments. For such a real-world environment $\psi_{\hat{\phi}}$ (parameterised by $\hat{\phi} = [\hat{\theta}, \mu_g]$), we apply *RAT* initial policy to transform the UPN policy conditioned by $\hat{\theta}$ to get the corrected real-world action a_t^R .

$$\begin{aligned} \forall_{\hat{\theta}}, |\hat{\theta} - \theta_g| &\leq \epsilon_{max} & (4) \\ a_t &\leftarrow \pi_{\hat{\theta}}^S(s_t) \\ \Delta a_t &\leftarrow \pi_{\theta_g, \mu_g}^{RAT}(s_t^{RAT} = [s_t, a_t]) \\ a_t^R &\leftarrow a_t + \Delta a_t \end{aligned}$$

The workflow of using *RAT* policy in adjacent environments is given in Algorithm 3.

Algorithm 3 Zero-shot sim-to-real policy transfer with *RAT* policy and UPN

Input:

- 1: $\psi_{\hat{\phi}}$ - real-world, $\psi_{\hat{\theta}}^{sim}$ - a parameterisable simulator
 - 2: π^S - a trained UPN for the task
 - 3: θ_g - ground-truth modellable parameters
 - 4: $\hat{\theta}$ - the adjacent environment parameters
 - 5: ϵ_{max} - the maximum allowed distance from the ground truth parameters
 - 6: **Output:** G^* - The zero-shot performance of *RAT* in the adjacent environment
 - 7:
 - 8: //Train the robust *RAT* initial policy
 - 9: $\bar{\pi}^{RAT} \leftarrow Train_RAT_Initial_Policy(\pi_{\theta_g}^S, \psi_{\theta_g}^{sim})$ Algo. 2
 - 10: //initialise *RAT* policy with $\bar{\pi}^{RAT}$
 - 11: $\pi_{\theta_g, \mu_g}^{RAT} \leftarrow \bar{\pi}^{RAT}$
 - 12: //apply *RAT* on adjacent environments
 - 13: **if** $|\hat{\theta} - \theta_g| \leq \epsilon_{max}$ **then**
 - 14: $a_t \leftarrow \pi_{\hat{\theta}}^S(s_t)$
 - 15: $\Delta a_t \leftarrow \pi_{\theta_g, \mu_g}^{RAT}(s_t^{RAT} = [s_t, a_t])$
 - 16: $G^* \leftarrow Evaluate\ a_t + \Delta a_t$ on adjacent environment (Eq. 4)
 - 17: **end if**
-

3.4 An Alternative *Supervised RAT* Model

The overall objective of *RAT* is to learn a mapping from the simulated action to its corresponding real-world action as given in Eq. 1. For this purpose, instead of using RL to learn a corrective action, we examine an alternative *supervised RAT* model where we learn a function $f : (s_t^R, s_{t+1}^R) \rightarrow a_t^R$ using supervised learning, where $s_t^R, s_{t+1}^R \in \mathcal{S}$ are two subsequent states in the real-world following the execution of action $a_t^R \in \mathcal{A}$ in the real-world. Then such a function f can be used to map two states

$s_t, s_{t+1} \in \mathcal{S}$ fetched from the simulator after executing UPN action $a_t \in \mathcal{A}$ to map the same real-world states to their corresponding real-world action $a_t^R, f(s_t, s_{t+1}) \rightarrow a_t^R$.

Supervised RAT has a relatively simpler formulation than *RAT*, which also makes it simpler to learn without requiring to calibrate RL specific hyperparameters. However, one drawback with *Supervised RAT* is that in the presence of large reality-gaps, supervised learning may not have seen simulation provided states (i.e., the ideal trajectory to follow) and thus not be able to learn the corresponding real-world action.

To apply *supervised RAT* model as a zero-shot learner, we follow the same hypothetical real-world setup discussed in Section 3.2 using the transition function Eq. 3. Then it is evaluated in adjacent environments as discussed in Section 3.3 by fetching a_t^R directly from f (Eq. 4).

4 Experiments

4.1 Experimental Setup

To empirically evaluate our approach, we adopt a set of six continuous control MuJoCo tasks – Ant, Half-Cheetah, Hopper, Humanoid, Swimmer and Walker2D (-v2), implemented with MuJoCo physics simulator [32]. For all tasks, we consider five latent parameters (mass of three body parts, friction and restitution) that determine the environment configuration, for which we fetch policies using pretrained UPNs.

To emulate simulated and real-world environments, for the purpose of this study, two instances of the same MuJoCo simulator are used, with the real-world environment instance differing from the simulated instance by virtue of a reality gap. To generate a significant reality-gap, we have used additional mass and friction for real-world body-parts of agents (+400%) similar to the approach taken by [19]. Such changes in latent parameters can be assumed to emulate factors such as air-resistance, muddy soil or rolling friction which may vary depending on the environment condition.

4.2 Training *RAT* Policy with UPN

We use an existing implementation of UPN¹ to store and fetch pretrained policies for MuJoCo tasks. To learn policies, the UPN is trained for 2×10^8 steps in the simulator using Proximal Policy Optimization (PPO) algorithm [28], uniformly sampling latent parameters to learn policies conditioned on a given set of parameters. To improve the policy at the ground truth latent parameters, we train another 5×10^6 steps conditioned on the ground truth parameters for all tasks except for Walker2D where 6×10^6 are used. These values were selected by examining the simulated task policy performance at each 1×10^6 steps, where we stop fine tuning the training if the improvement is less than 5%, which we consider as a criterion to determine that the simulated task policy has reached convergence.

With the trained UPN, we train both robust *RAT* initial policy and *Supervised RAT* using 1×10^6 simulated steps by uniformly sampling normalised mass and friction

¹https://github.com/VincentYu68/policy_transfer

	Transfer	DR	<i>Supervised RAT</i>	<i>RAT</i>
Ant	-0.0363 ± 0.0021	-0.0372 ± 0.0019	0.6374 ± 0.0015	0.228 ± 0.0016
Half-Cheetah	0.8607 ± 0.0049	0.8628 ± 0.0057	0.8752 ± 0.0001	0.8817 ± 0.0011
Hopper	1.6402 ± 0.0168	1.6531 ± 0.0169	1.6620 ± 0.0193	1.7263 ± 0.0221
Humanoid	4.9787 ± 0.0101	4.9841 ± 0.0114	5.2504 ± 0.0004	5.0845 ± 0.0124
Swimmer	0.0401 ± 0.0006	0.0399 ± 0.0006	0.0208 ± 0.0007	0.0436 ± 0.0005
Walker2D	0.8282 ± 0.0002	0.8348 ± 0.0028	0.4768 ± 0.013	0.8077 ± 0.008

Table 1: The zero-shot transfer performance (average step-wise cumulative reward) of *RAT* policy and *Supervised RAT* against baselines in six MuJoCo environments. Performance is evaluated on 100 episodes with a horizon of 500 steps (\pm std. error).

values in the range of $[0, 3)$ and $[0, 1)$, respectively, from which the reality-gap is determined by subtracting the normalised ground truth parameter value. Here, we use a relatively substantial mass range because of our use of a high mass based reality gap. In reality, the sampled value range could be determined based on the domain knowledge of the reality-gap (e.g., wind speed, clay soil stickiness, etc.). Specifically, for each episode of a task we sample a new reality-gap value and add it to the original ground truth latent value to generate the new value, which is used to govern the transition function. Table 1 shows the average step-wise cumulative reward of *RAT* initialised with the trained initial policy when used in the real-world without any additional real-world training (i.e., zero-shot transfer performance). We also present the performance of the alternative *Supervised RAT* model trained to directly map simulation trajectory to real-world actions that would yield a similar trajectory in the real-world.

We use the following UPN-based baselines to compare *RAT* with.

- Transfer policy: The simulated policy from UPN conditioned by the true latent parameter values is transferred to the real-world without any additional training in the real-world. We evaluate the policy performance using 100 episodes in the real-world.
- Domain Randomised (DR) policy: 10 latent parameters $\pm 5\%$ from the ground truth are sampled, for each of which the UPN is conditioned to fetch the simulated policy and averaged to obtain a final policy. This generalised DR policy is then applied to the real-world and evaluated similar to the transfer policy.

To compensate for the 1×10^6 simulation steps required for training the *RAT* initial policy, both transfer and DR policies are trained for an equal amount of additional steps in the simulator.

4.3 Performance in Adjacent Environments

We use the *RAT* policy hyperparameter tuned to a real-world setting to examine its applicability when the latent parameters deviate from the original ground truth values. For this purpose, we uniformly sample 100 latent parameters, deviating $\pm 5\%$ from the ground truth latent parameter values and apply the *RAT* policy, without any additional

	Transfer	DR	<i>Supervised RAT</i>	<i>RAT</i>
Ant	-0.0372 \pm 0.0004	-0.0372 \pm 0.0004	0.6346 \pm 0.0009	0.2288 \pm 0.0011
Half-Cheetah	0.8541 \pm 0.0016	0.857 \pm 0.0015	0.8752 \pm 0.0000	0.8749 \pm 0.001
Hopper	1.6532 \pm 0.0004	1.6519 \pm 0.0004	1.6614 \pm 0.0004	1.7548 \pm 0.0006
Humanoid	4.9964 \pm 0.0019	4.9971 \pm 0.0021	5.2443 \pm 0.0008	5.0791 \pm 0.0021
Swimmer	0.0394 \pm 0.0002	0.0391 \pm 0.0002	0.0209 \pm 0.0003	0.0416 \pm 0.0002
Walker2D	0.919 \pm 0.0177	0.8459 \pm 0.005	0.4716 \pm 0.003	0.8056 \pm 0.003

Table 2: The zero-shot adaptation performance (average step-wise cumulative reward) of *RAT* policy and *Supervised RAT* for 100 uniformly sampled latent parameter configurations deviating $\pm 5\%$ from the original ground truth values. Performance is evaluated on 100 episodes with a horizon of 500 steps (\pm std. error).

training, to transform the UPN policy conditioned on each of the sampled latent values to ground-truth conditions set to the same sampled latent values. Table 2 shows the average step-wise cumulative reward of *RAT* policy on these adjacent latent parameter configurations.

These results illustrate that *RAT* policy is robust to a degree of deviation from the original ground truth values. While *Supervised RAT* performs better in environments such as Ant and Humanoid, it shows collapses in performance compared to the baselines in Swimmer and Walker2D, likely because of not having seen target simulation trajectories in the real-world training data. In contrast, *RAT* policy shows stable and improved performance compared to the baselines, perhaps due to better exploration provided by RL. In the Walker2D environment, *RAT* performs marginally poorer than the baselines which could be due to the unavailability of a policy in the real-world to imitate the simulated policy. However, in general, these results demonstrate that when a simulated task-specific policy has converged in the simulator, training *RAT* with a small number of additional simulated experience can be beneficial as a sim2real zero-shot transfer policy when compared to the baselines.

5 Conclusion

In this study, we have proposed a novel policy transformation approach for adaptable sim2real transfer on unseen environments. The proposed approach, *Reverse Action Transformation (RAT)*, learns a policy to correct real-world policies such that the resulting trajectory closely follows the trajectory corresponding to a trained simulated policy. This learnt correction policy is then deployed in unseen real-world environments in conjunction with the corresponding simulated policies from a UPN to achieve zero-shot adaptation. We have empirically evaluated our approach in six MuJoCo tasks, and demonstrated its superior performance as a zero-shot learner compared to the relevant baselines.

References

- [1] Abbeel, P., Quigley, M., Ng, A.Y.: Using inaccurate models in reinforcement learning. In: Proceedings of the 23rd International Conference on Machine Learning. pp. 1–8. ICML '06, Association for Computing Machinery, New York, NY, USA (2006). <https://doi.org/10.1145/1143844.1143845>, <https://doi.org/10.1145/1143844.1143845>
- [2] Ajay, A., Bauza, M., Wu, J., Fazeli, N., Tenenbaum, J.B., Rodriguez, A., Kaelbling, L.P.: Combining physical simulators and Object-Based networks for control. In: 2019 International Conference on Robotics and Automation (ICRA). pp. 3217–3223 (May 2019)
- [3] Ajay, A., Wu, J., Fazeli, N., Bauza, M., Kaelbling, L.P., Tenenbaum, J.B., Rodriguez, A.: Augmenting physical simulators with stochastic neural networks: Case study of planar pushing and bouncing. In: 2018 IEEE/RSJ International Conference on Intelligent Robots and Systems (IROS). pp. 3066–3073 (Oct 2018)
- [4] Akkaya, I., Andrychowicz, M., Chociej, M., Litwin, M., McGrew, B., Petron, A., Paino, A., Plappert, M., Powell, G., Ribas, R., et al.: Solving rubik’s cube with a robot hand. arXiv preprint arXiv:1910.07113 (2019)
- [5] Allevato, A., Short, E.S., Pryor, M., Thomaz, A.: Tunenet: One-shot residual tuning for system identification and sim-to-real robot task transfer. In: Conference on Robot Learning. pp. 445–455. PMLR (2020)
- [6] Allevato, A.D., Schaertl Short, E., Pryor, M., Thomaz, A.L.: Iterative residual tuning for system identification and sim-to-real robot learning. *Autonomous Robots* **44**(7), 1167–1182 (2020). <https://doi.org/10.1007/s10514-020-09925-w>, <https://doi.org/10.1007/s10514-020-09925-w>
- [7] Ba, Y., Zhao, G., Kadambi, A.: Blending diverse physical priors with neural networks (Oct 2019)
- [8] Chebotar, Y., Handa, A., Makoviychuk, V., Macklin, M., Issac, J., Ratliff, N.D., Fox, D.: Closing the sim-to-real loop: Adapting simulation randomization with real world experience. In: International Conference on Robotics and Automation, ICRA 2019, Montreal, QC, Canada, May 20-24, 2019. pp. 8973–8979. IEEE (2019). <https://doi.org/10.1109/ICRA.2019.8793789>, <https://doi.org/10.1109/ICRA.2019.8793789>
- [9] Desai, S., Karnan, H., Hanna, J.P., Warnell, G., a. P. Stone: Stochastic grounded action transformation for robot learning in simulation. In: 2020 IEEE/RSJ International Conference on Intelligent Robots and Systems (IROS). pp. 6106–6111 (2020). <https://doi.org/10.1109/IROS45743.2020.9340780>
- [10] Desai, S., Durugkar, I., Karnan, H., Warnell, G., Hanna, J., Stone, P.: An imitation from observation approach to transfer learning with dynamics mismatch. In: Larochelle, H., Ranzato, M., Hadsell, R., Balcan, M., Lin, H.

- (eds.) *Advances in Neural Information Processing Systems 33: Annual Conference on Neural Information Processing Systems 2020, NeurIPS 2020, December 6-12, 2020, virtual (2020)*, <https://proceedings.neurips.cc/paper/2020/hash/28f248e9279ac845995c4e9f8af35c2b-Abstract.html>
- [11] Du, Y., Watkins, O., Darrell, T., Abbeel, P., Pathak, D.: Auto-tuned sim-to-real transfer. arXiv preprint arXiv:2104.07662 (2021)
 - [12] Farchy, A., Barrett, S., MacAlpine, P., Stone, P.: Humanoid robots learning to walk faster: From the real world to simulation and back. In: *AAMAS*. pp. 39–46 (2013)
 - [13] Golemo, F., Taiga, A.A., Courville, A., Oudeyer, P.Y.: Sim-to-real transfer with neural-augmented robot simulation. In: Billard, A., Dragan, A., Peters, J., Morimoto, J. (eds.) *Proceedings of The 2nd Conference on Robot Learning. Proceedings of Machine Learning Research*, vol. 87, pp. 817–828. PMLR (29–31 Oct 2018), <https://proceedings.mlr.press/v87/golemo18a.html>
 - [14] Hanna, J.P., Desai, S., Karnan, H., Warnell, G., Stone, P.: Grounded action transformation for sim-to-real reinforcement learning. *Machine Learning* **110**(9), 2469–2499 (2021)
 - [15] Hanna, J.P., Stone, P.: Grounded action transformation for robot learning in simulation. In: *AAAI*. pp. 4931–4932. AAAI Press (2017)
 - [16] Heidrich-Meisner, V., Igel, C.: Hoeffding and bernstein races for selecting policies in evolutionary direct policy search. In: *Proceedings of the 26th Annual International Conference on Machine Learning*. pp. 401–408. ICML '09, Association for Computing Machinery, New York, NY, USA (2009). <https://doi.org/10.1145/1553374.1553426>, <https://doi.org/10.1145/1553374.1553426>
 - [17] Jiang, Y., Zhang, T., Ho, D., Bai, Y., Liu, C.K., Levine, S., Tan, J.: Simgan: Hybrid simulator identification for domain adaptation via adversarial reinforcement learning. *CoRR* **abs/2101.06005** (2021), <https://arxiv.org/abs/2101.06005>
 - [18] Johannink, T., Bahl, S., Nair, A., Luo, J., Kumar, A., Loskyll, M., Ojea, J.A., Solowjow, E., Levine, S.: Residual reinforcement learning for robot control. In: *2019 International Conference on Robotics and Automation (ICRA)*. pp. 6023–6029 (May 2019)
 - [19] Karnan, H., Desai, S., Hanna, J.P., Warnell, G., Stone, P.: Reinforced grounded action transformation for sim-to-real transfer. In: *2020 IEEE/RSJ International Conference on Intelligent Robots and Systems (IROS)*. pp. 4397–4402. IEEE (2020)
 - [20] Li, J.K., Lee, W.S., Hsu, D.: Push-net: Deep planar pushing for objects with unknown physical properties. In: Kress-Gazit, H., Srinivasa, S.S., Howard, T., Atanasov, N. (eds.) *Robotics: Science and Systems*

- XIV, Carnegie Mellon University, Pittsburgh, Pennsylvania, USA, June 26-30, 2018 (2018). <https://doi.org/10.15607/RSS.2018.XIV.024>, <http://www.roboticsproceedings.org/rss14/p24.html>
- [21] Matas, J., James, S., Davison, A.J.: Sim-to-real reinforcement learning for deformable object manipulation. In: Conference on Robot Learning. pp. 734–743. PMLR (2018)
- [22] Mnih, V., Kavukcuoglu, K., Silver, D., Rusu, A.A., Veness, J., Bellemare, M.G., Graves, A., Riedmiller, M., Fidjeland, A.K., Ostrovski, G., et al.: Human-level control through deep reinforcement learning. *nature* **518**(7540), 529–533 (2015)
- [23] Mozian, M., Higuera, J.C.G., Meger, D., Dudek, G.: Learning domain randomization distributions for training robust locomotion policies. In: 2020 IEEE/RSJ International Conference on Intelligent Robots and Systems (IROS). pp. 6112–6117. IEEE
- [24] Muratore, F., Eilers, C., Gienger, M., Peters, J.: Data-efficient domain randomization with bayesian optimization. *IEEE Robotics Autom. Lett.* **6**(2), 911–918 (2021). <https://doi.org/10.1109/LRA.2021.3052391>, <https://doi.org/10.1109/LRA.2021.3052391>
- [25] Rajeswaran, A., Ghotra, S., Ravindran, B., Levine, S.: Epopt: Learning robust neural network policies using model ensembles. In: 5th International Conference on Learning Representations, ICLR 2017, Toulon, France, April 24–26, 2017, Conference Track Proceedings. OpenReview.net (2017), <https://openreview.net/forum?id=SyWvgP5el>
- [26] Ramos, F., Possas, R., Fox, D.: Bayessim: Adaptive domain randomization via probabilistic inference for robotics simulators. In: Bicchi, A., Kress-Gazit, H., Hutchinson, S. (eds.) *Robotics: Science and Systems XV*, University of Freiburg, Freiburg im Breisgau, Germany, June 22–26, 2019 (2019). <https://doi.org/10.15607/RSS.2019.XV.029>, <https://doi.org/10.15607/RSS.2019.XV.029>
- [27] Sadeghi, F., Levine, S.: CAD2RL: real single-image flight without a single real image. In: Amato, N.M., Srinivasa, S.S., Ayanian, N., Kuindersma, S. (eds.) *Robotics: Science and Systems XIII*, MIT, USA, 2017 (2017)
- [28] Schulman, J., Wolski, F., Dhariwal, P., Radford, A., Klimov, O.: Proximal policy optimization algorithms. *CoRR* **abs/1707.06347** (2017), <http://arxiv.org/abs/1707.06347>
- [29] Sheckells, M., Garimella, G., Mishra, S., Kobilarov, M.: Using data-driven domain randomization to transfer robust control policies to mobile robots. In: 2019 International Conference on Robotics and Automation (ICRA). pp. 3224–3230 (2019). <https://doi.org/10.1109/ICRA.2019.8794343>
- [30] Silver, T., Allen, K., Tenenbaum, J., Kaelbling, L.: Residual policy learning (Dec 2018)

- [31] Tobin, J., Fong, R., Ray, A., Schneider, J., Zaremba, W., Abbeel, P.: Domain randomization for transferring deep neural networks from simulation to the real world. In: 2017 IEEE/RSJ International Conference on Intelligent Robots and Systems (IROS). pp. 23–30 (2017)
- [32] Todorov, E., Erez, T., Tassa, Y.: Mujoco: A physics engine for model-based control. In: 2012 IEEE/RSJ International Conference on Intelligent Robots and Systems. pp. 5026–5033. IEEE (2012)
- [33] Yu, W., Kumar, V.C., Turk, G., Liu, C.K.: Sim-to-real transfer for biped locomotion. In: Proc. of The International Conference on Intelligent Robots and Systems (IROS) (2019)
- [34] Yu, W., Liu, C.K., Turk, G.: Policy transfer with strategy optimization. In: International Conference on Learning Representations (2019), <https://openreview.net/forum?id=H1g6osRcFQ>
- [35] Yu, W., Tan, J., Liu, C.K., Turk, G.: Preparing for the unknown: Learning a universal policy with online system identification. In: Amato, N.M., Srinivasa, S.S., Ayanian, N., Kuindersma, S. (eds.) Robotics: Science and Systems XIII, Massachusetts Institute of Technology, Cambridge, Massachusetts, USA, July 12-16, 2017 (2017). <https://doi.org/10.15607/RSS.2017.XIII.048>, <http://www.roboticsproceedings.org/rss13/p48.html>
- [36] Zeng, A., Song, S., Lee, J., Rodriguez, A., Funkhouser, T.: Tossingbot: Learning to throw arbitrary objects with residual physics. *IEEE Transactions on Robotics* **36**(4), 1307–1319 (2020). <https://doi.org/10.1109/TRO.2020.2988642>
- [37] Zhang, G., Zhong, L., Lee, Y., Lim, J.J.: Policy transfer across visual and dynamics domain gaps via iterative grounding. In: Shell, D.A., Toussaint, M., Hsieh, M.A. (eds.) Robotics: Science and Systems XVII, Virtual Event, July 12-16, 2021 (2021). <https://doi.org/10.15607/RSS.2021.XVII.006>, <https://doi.org/10.15607/RSS.2021.XVII.006>
- [38] Zhu, S., Kimmell, A., Bekris, K.E., Boularias, A.: Fast model identification via physics engines for data-efficient policy search. In: Proceedings of the 27th International Joint Conference on Artificial Intelligence. pp. 3249–3256. IJCAI’18, AAAI Press (2018)